

Power Emission Density-Based Interference Analysis for Random Wireless Networks

Minming Ni^{*†}, Jianping Pan^{*}, Lin Cai^{*}

^{*}University of Victoria, Victoria, BC, Canada

[†]State Key Lab. of Rail Traffic Control and Safety, Beijing Jiaotong University, Beijing, China

Email:{mmni, pan}@uvic.ca, cai@ece.uvic.ca

Abstract—To reduce the difficulties in calculating the aggregated interference power at an observed receiver, a Power Emission Density-based analysis method is proposed in this paper. By utilizing the new method, the traditional discrete-style calculation (i.e., obtain each concurrent interferer’s impact on the observed receiver individually, and add them together) can be replaced with a concise integration over the entire network area, which could effectively reduce the complexity of interference-related studies. The accuracy of the proposed method is verified by extensive simulations in different network scenarios. The results and analytical methods given in this paper will lead to a series of geometrical-based studies on the interference in random wireless networks, which could be used to guide the design and implementation of large-scale wireless networks.

I. INTRODUCTION

Due to the broadcast nature of the wireless medium, the signal received at a receiver is usually a distorted version of the desired transmission superimposed with other undesired or interfering signals transmitted nearby. For a network with the centralized structure (e.g., the cellular networks with base stations), such interference can usually be effectively mitigated by applying some global scheduling/optimizing schemes, or implementing some sophisticated multi-user detection or interference cancellation algorithms. However, for the decentral-ized random networks (e.g., ad hoc networks, sensor networks, and cognitive networks), the decisions for network operations (e.g., medium access control, routing, and topology control) are always made by each network terminal in a distributed way, which means the interference might not be tightly controllable, and could severely affect the entire network’s performance [1]. Therefore, appropriate modeling and accurate characterization of interference will be vital for both the design and implementation of random wireless networks. Currently, a myriad of interference-related research work for random wireless networks is already available in the literature [2]. Although these results are different with regard to their intended applications, abstract levels, or expression forms, they can still be roughly categorized into two classes according to their focuses.

For the first class of the interference-related research, its major concern is given to the *statistical characteristics of interference in the network*, which can be expressed in terms of probability density functions involved with the propagation model, interferer spatial model, medium access model, and traffic model. In this category, if the exact information of the network nodes’ location is not available, the homogenous

Poisson Point Process (PPP) $\Phi = \{X_i\}$ is a commonly used assumption [3], [4], where X_i is the location of the i -th terminal. By utilizing a distance-dependent fading model to describe the interference power measured at a given receiver, the aggregated interference can be represented as the *shot noise* associated with Φ , which follows an α -stable distribution under certain conditions [5]. Based on the unique features of PPP and shot noise, a series of research work had appeared in the last few years [6]. However, although the homogenous PPP assumption is analytically convenient, as it results in elegant and tractable expressions (and even closed-form expressions in some particular cases), it may not be a valid assumption in the practical situations [7]. For example, the practical networks are always deployed within finite regions, which means that the network could not be treated as homogenous for the terminals near the network boundary; and the terminal distribution in the real world is not purely random, as the exclusive regions created by CSMA/CA scheme always lead to more regular interferer location distributions.

For the second class of the interference-related study, the emphasis is moved to the *effect of interference on the network performances*. Among all the models used in this category, the protocol interference model and the physical interference model are the two most typical ones, which were proposed in [8]. The protocol interference model is based on the vulnerability circle capture model [9] and defines a condition for successful communications between a single node pair. By applying this condition on all the concurrent node pairs in the network, capacity bounds can be obtained for different network settings. On the other hand, the physical interference model, which is based on the power capture model [10], focuses on the effect of the aggregated interference from all the other transmitters. Although the protocol interference model successfully abstracts several aspects of wireless communications, it is widely accepted that the physical interference model is more realistic and accurate. However, the much higher complexity, which is caused by calculating the sum of all the undesired signals, might still prevent the application of the physical interference model on large and complicated network scenarios.

According to the above brief investigation on the existing tools or methods used for interference analysis, it is interesting to find out that the *discrete-style* calculation for the aggregated interference (i.e., calculate each concurrent interferer’s impact

on the observed receiver individually, and add them together) is the basic but also one of the major obstacles for obtaining accurate and easy to be used interference models. To solve this problem, a Power Emission Density (PED)-based interference analysis method is proposed in this paper, which is inspired by the natural relationship between summation and integral, and its extensive applications in both physics and astronomy (e.g., [11]). The basic idea of the new method is to equal the effect of a single terminal's transmission power to the effect generated by the power emitted within the exclusive region created by the transmitter and its receiver. In this way, the difficult discrete calculation can be replaced with a concise integral over the network region, which is recognized as the *continuous-style* method. By utilizing the new method, the commonly used regular network area model (e.g., square, hexagon, and disk) can be extended to any more realistic irregular shape. Moreover, the information of node location or exclusive region arrangement, which is known as the difficult circle/sphere packing problem in geometry [12], is no longer needed, so the complexity of interference-related studies could also be greatly reduced.

The remainder of the paper is organized as follows. The system model for explaining our new method is given in Section II. The basic idea and method for PED are explained in detail in Section III. Three different network scenarios are used to verify the accuracy of the proposed method in Section IV, followed by a brief discussion about some possible applications and improvements of the PED-based interference analysis method in Section V. Finally, Section VI concludes this paper.

II. SYSTEM MODEL

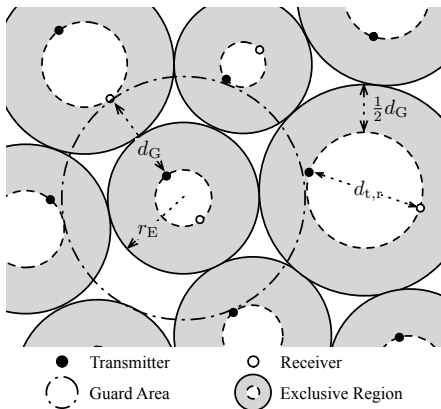


Fig. 1. Guard area and the exclusive regions

For general modeling, it is assumed that the observed random network is densely deployed within a finite region \mathcal{S}_N . Due to the lack of centralized network infrastructures, all the network nodes transmit their packets with a fixed transmission power P_t . Moreover, we assume that a communication link will only be established when the distance $d_{t,r}$ between the transmitter and the receiver is shorter than the predefined

maximum transmission range d_{max} , which is determined by P_t and the total interference level in the network. Due to the fact that the concurrent transmissions may generate considerable accumulated interference to each other, a fixed guard distance d_G is maintained for each communicating pair to shape an exclusive region (ER) respectively, within which only one active communicating pair can exist. As shown in Fig. 1, the radius r_E of an ER is changed with $d_{t,r}$, and $r_E = \frac{1}{2}(d_{t,r} + d_G)$. For simplicity, the power of the dedicated signal received at distance d away from the transmitter is modeled with a general path loss model as $P_r = \beta P_t / d^\eta$, where β is a constant determined by the hardware features of the transceivers, and η is the path loss exponent depending on the propagation environment.

III. POWER EMISSION DENSITY

For a communicating pair, as long as their inter-distance $d_{t,r}$ and the middle point of their line segment remain the same, the ER of this node pair remains the same no matter what kind of relative positions the two nodes are. Therefore, as shown in Fig. 2, once an ER is given, the expectation of the emitted signal power received at an observation point (OP), which is located with distance x_o ($x_o > r_E$) away from the ER's center, can be calculated as

$$\overline{P_{r,OP}} = \frac{1}{2\pi} \int_0^{2\pi} \frac{\beta P_t}{\sqrt{((d_{t,r}/2)^2 - d_{t,r} x_o \cos \theta + x_o^2)^\eta}} d\theta. \quad (1)$$

Although the above integral can be obtained for the typical values of η by referring to [13]¹, to avoid over complicated mathematical expressions, we will only consider the situation of $\eta = 2$ in the following parts of this paper, but the same method could also be applied for other channel conditions. Hence, $\overline{P_{r,OP}}$ can be obtained as

$$\overline{P_{r,OP}} = \frac{\beta P_t}{x_o^2 - d_{t,r}^2}, \quad \text{for } x_o > r_E. \quad (2)$$

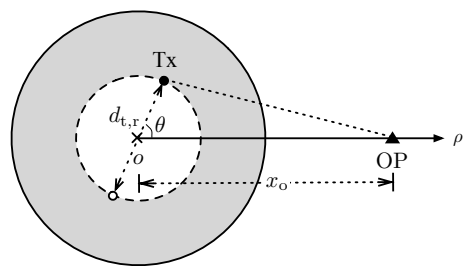


Fig. 2. Calculation for the expectation of received signal power at OP

On the other hand, the effect of a single *point transmitter* calculated above can also be equivalent to an *area transmitter* with constant power emission density (PED) λ (W/m²). If we assume the shape and the size of the imaginary area

¹For example, **2.575** can be used for $\eta = 3$ and 5, **2.554-3** is helpful for both $\eta = 4$ and 6.

transmitter are identical to the ER created by the observed point transmitter and receiver, the received power $P'_{r,OP}$ at the OP could be calculated by the infinitesimal method shown in Fig. 3 as

$$\begin{aligned} P'_{r,OP} &= \iint_{S_E} \frac{\beta\lambda dS}{d_{OP}^2} = \int_0^{r_E} \int_0^{2\pi} \frac{\beta\lambda r d\theta}{r^2 - 2x_o r \cos\theta + x_o^2} dr \\ &= \pi\beta\lambda \ln \frac{x_o^2}{x_o^2 - r_E^2}, \end{aligned} \quad (3)$$

where S_E is the ER of the communicating pair. By equalizing (2) and (3), the PED λ can be obtained as (for $\eta = 2$, and S_E is a disk with radius r_E)

$$\lambda = \frac{P_t}{\pi \ln \frac{x_o^2}{x_o^2 - r_E^2} (x_o^2 - d_{t,r}^2)}. \quad (4)$$

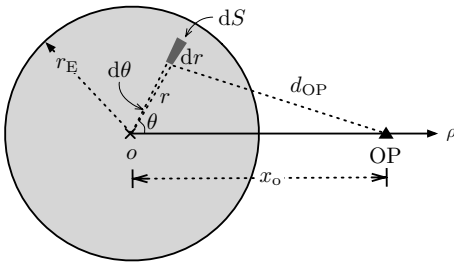


Fig. 3. Illustration for the power emission density-based calculation

According to the above formula, once a communicating pair is given, the equivalent PED will not have obvious change when x_o is relatively large. Therefore, we should be able to find an accurate enough approximation of λ as $\hat{\lambda} = \lambda|_{x_o=kr_E}$, then the approximation error Δ is

$$\Delta = \left| \frac{P'_{r,OP}|_{\lambda=\hat{\lambda}} - \overline{P'_{r,OP}}}{\overline{P'_{r,OP}}} \right| = \left| \frac{\ln \frac{x_o^2}{x_o^2 - r_E^2} \cdot (x_o^2 - d_{t,r}^2)}{\ln \frac{k^2}{k^2 - 1} \cdot (k^2 r_E^2 - d_{t,r}^2)} - 1 \right|. \quad (5)$$

In Fig. 4, the approximation error Δ is demonstrated with fixed r_E , varied $d_{t,r}$ and k . Generally, Δ decreases from a initial value to zero first, after that, it increases with x_o to a relatively stable state. When k is fixed, larger $d_{t,r}$ leads to smaller dynamic range of Δ . When $d_{t,r}$ is fixed, k 's change will affect the location of Δ 's zero points.

By comparing the results of the approximation error analysis with their physical meanings, some interesting results could be found. First, considering that the signal power is faded with the power law mentioned in the system model, the observed transmitter may only generate obvious effect on the first few layers of receivers around it. Therefore, it should be guaranteed that the approximated results for these receivers can still have high accuracy. On the other hand, for the receivers far away from the observed ER, due to the fact that the actual values of the reception power are already very small, the slightly increased estimation error will not greatly affect the accuracy of related analysis. In other words, the selection of k 's value

should consider both the effects before and after Δ 's zero point. Combining the system model, the first layer of receivers near the observed ER should have distance around $2r_E$, then we could summarize a theorem as follow.

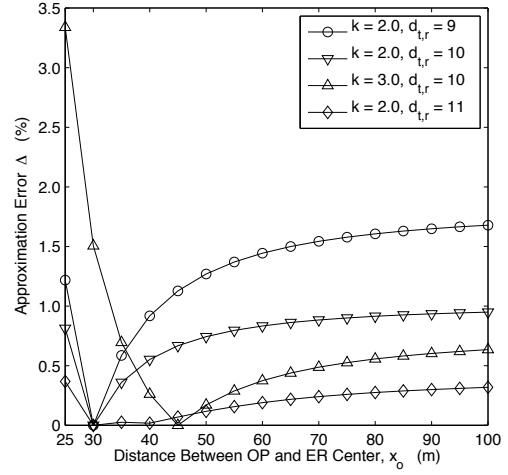


Fig. 4. Approximation error Δ with different $d_{t,r}$ and k ($r_E = 15$)

Theorem of PED. For a node pair occupying an ER S_E , its transmission power P_t could be approximated as uniformly emitted inside the ER with density λ for an observation point with distance x_o away from the ER center, where

$$\lambda \triangleq \frac{P_t}{(x_o^2 - d_{t,r}^2) \iint_{S_E} \frac{dx dy}{(x-x_o)^2 + y^2}} \quad \text{for } \eta = 2.$$

To simplify its utilization, λ could be approximated by

$$\hat{\lambda} = \lambda|_{x_o=kr_E}.$$

The value of k could be set to 2 for common use, but can also be further tuned to satisfy different accurate requirements.

By applying the above theorem, the accumulated interference power at a specific receiver can be obtained in a simple continuous way as the following corollary.

Corollary 1. Given a network with PED λ and deploying region S_N , the aggregated interference, which is generated by all the concurrent communicating pairs in the network, accumulated at a receiver with coordinates (x_o, y_o) and ER S_E can be calculated as

$$P_r^{\text{PED}}(x_o, y_o) = \beta\lambda \iint_{S_N - S_E} \frac{dx dy}{(x-x_o)^2 + (y-y_o)^2}. \quad (6)$$

Note that, by properly setting the origin of the coordinate system (e.g., move the observed receiver to $(0, 0)$), the integral in (6) can be greatly simplified.

IV. ACCURACY EVALUATION

In this section, the PED-based interference analysis method will be evaluated by three different network examples. For easy

calculation, we let $P_t = 1$ W, $\beta = 1$, $d_{\max} = \frac{d_G}{2} = 10$ m, so $r_E = 15$ m. The varying of the network area will change the total number of ERs could be arranged into the network. By utilizing the PED-based method, the accumulated interference at a specific position could be obtained without knowing the details of all the communicating node pairs' position, which is relatively easier to be handled than the traditional discrete calculation method.

A. Square Network Area with Square Grid ERs

We first consider a square network, within which all the network nodes are communicating with $d_{t,r} = d_{\max}$, so the size of each ER is the same. Moreover, we assume that the ERs are arranged in a square grid as shown in Fig. 5, so the network region \mathcal{S}_N can just be arranged with L_S layers of ERs (L_S is a natural number), which means $\sqrt{\|\mathcal{S}_N\|}/(2r_E) = L_S$, where $\|\mathcal{S}_N\|$ represent the area of the network region.

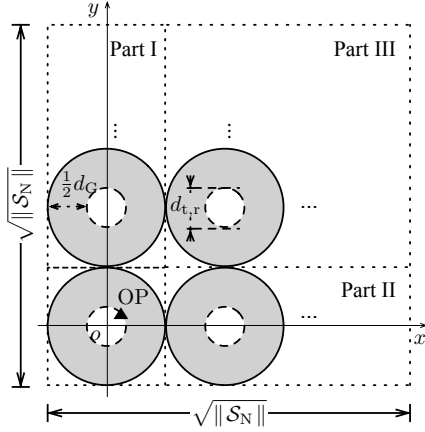


Fig. 5. Square network with ERs arranged as a square grid

By utilizing the Monte Carlo method, the expected total interference power accumulated at the observed receiver, which is randomly located on the boundary of circle $x^2 + y^2 = \frac{1}{4}d_{t,r}^2$, as shown in Fig. 5, can be obtained by repeating a large number of simulation rounds. Although the simulation is easy to be carried, the closed-form expression of the accumulated interference can never be obtained by this method.

However, if we turn to the PED-based method, it is clear that, $\|\mathcal{S}_E\| = 4r_E^2$ in the square grid network, and the interference accumulated at the origin $(0,0)$ can be calculated in three parts as labeled in Fig. 5. Due to the symmetry, the interference generated by ERs located in network area Part I and Part II are the same, therefore,

$$\begin{aligned} P_{r,SG}^{\text{PED}}(0,0) &= 2P_{r,SG-I}^{\text{PED}}(0,0) + P_{r,SG-III}^{\text{PED}}(0,0) \\ &= 2\beta\lambda \int_{-r_E}^{r_E} \int_{r_E}^{\sqrt{\|\mathcal{S}_N\|}-r_E} \frac{dx dy}{x^2 + y^2} \\ &\quad + \beta\lambda \int_{r_E}^{\sqrt{\|\mathcal{S}_N\|}-r_E} \int_{r_E}^{\sqrt{\|\mathcal{S}_N\|}-r_E} \frac{dx dy}{x^2 + y^2}. \end{aligned} \quad (7)$$

The closed-form expression of $P_{r,SG}^{\text{PED}}(0,0)$ can be finally obtained by combining the Theorem of PED and the following

two integration formulas:

$$\int \frac{1}{x^2 + a^2} dx = \frac{\arctan\left(\frac{x}{a}\right)}{a} + C, \quad (8)$$

$$\int \frac{\arctan\left(\frac{a}{x}\right)}{x} dx = -\frac{i\left(\text{Li}_2\left(-\frac{ai}{x}\right) - \text{Li}_2\left(\frac{ai}{x}\right)\right)}{2} + C, \quad (9)$$

where a and C are constants, $\text{Li}_n(\cdot)$ is the polylogarithm function, and i is the imaginary unit.

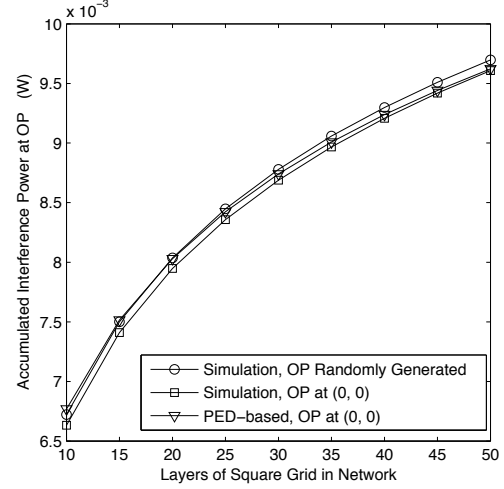


Fig. 6. Numerical and simulation results of square network with square grid, (the randomly generated OP is on circle $x^2 + y^2 = \frac{1}{4}d_{t,r}^2$, shown in Fig. 5)

The numerical results of $P_{r,SG}^{\text{PED}}(0,0)$ are illustrated in Fig. 6 with changed L_S , which represents different $\|\mathcal{S}_N\|$. Meanwhile, both the simulation results of the expected total interference power accumulated at the random receiver within the observed ER and the origin $(0,0)$ are also demonstrated. By comparing these results, some direct conclusions could be obtained as follow. First, the total interference power accumulated at OP has an obvious increase with a larger network area. Second, the accuracy of PED-based calculation is acceptable. For example, when $\|\mathcal{S}_N\| = 81 \times 10^4$ m² ($L_S = 30$ m), the error between $P_{r,SG}^{\text{PED}}(0,0)$ and the simulation results for OP at $(0,0)$ is about 0.6%; when $\|\mathcal{S}_N\|$ grows to 144×10^4 m² ($L_S = 40$ m), the error further reduces to only about 0.3%. Third, the difference between the total interference power accumulated at $(0,0)$ and the observed receiver's random position is also very small (e.g., the average error is less than 1%), therefore, we could have the corollary below to simplify some related calculations.

Corollary 2. For a large network, the total interference power accumulated at a receiver can be approximated by the interference power accumulated at the center of the observed node pair's ER.

B. Rectangle Network Area with Hexagon Grid ERs

If all the ERs in the network are arranged in the most compact way [12], a rectangle network with a hexagon grid will be shaped as shown in Fig. 7. Similar as the previous

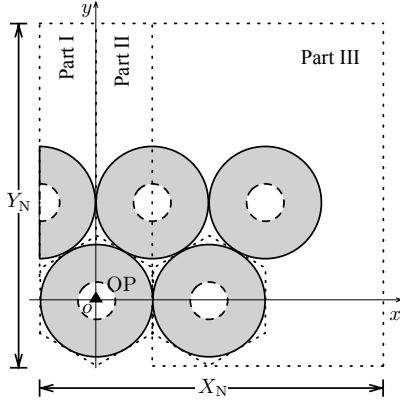


Fig. 7. Rectangle network with ERs arranged as a hexagon grid

situation, we still assume that the network area can just fit L_H layers of ERs (L_H is a natural number), which means $X_N/(2r_E) = Y_N/\left(\frac{2\sqrt{3}r_E}{3}\right) = L_H$, and $\|\mathcal{S}_N\| = X_N \cdot Y_N$. Correspondingly, the total interference power accumulated at the origin $P_{r,\text{HG}}^{\text{PED}}(0,0)$, can be calculated similarly in three parts as labeled in Fig. 7,

$$\begin{aligned} P_{r,\text{HG}}^{\text{PED}}(0,0) &= 2P_{r,\text{HG-I}}^{\text{PED}}(0,0) + P_{r,\text{HG-III}}^{\text{PED}}(0,0) \\ &= 2\beta\lambda \int_{-r_E}^0 \int_{\frac{\sqrt{3}}{3}x + \frac{2\sqrt{3}}{2}r_E}^{Y_N - \frac{2\sqrt{3}}{2}r_E} \frac{dx dy}{x^2 + y^2} \\ &\quad + \beta\lambda \int_{r_E}^{X_N - 2r_E} \int_{-\frac{2\sqrt{3}}{2}r_E}^{Y_N - \frac{2\sqrt{3}}{2}r_E} \frac{dx dy}{x^2 + y^2}. \end{aligned} \quad (10)$$

The closed-form expression of $P_{r,\text{HG}}^{\text{PED}}(0,0)$ can also be finally obtained by referring to (8) and (9).

In Fig. 8, the numerical results of $P_{r,\text{HG}}^{\text{PED}}(0,0)$, the simulation results of the accumulated interference power at randomly located receiver and $(0,0)$ are all demonstrated with different L_H . Similarly, the accuracy of the PED-based approach and the correctness of Corollary 2 are validated. Comparing with the results in Fig. 6, the hexagon grid accumulates much higher interference at the OP with the same number of grid layers, and this is due to that more compact arrangement reduces the distances between interfering nodes.

In fact, $P_{r,\text{HG-I}}^{\text{PED}}(0,0)$ in (10) can also be approximated by simply replacing the hexagon region by the disk ER with radius r_E as

$$P_{r,\text{HG-I}}^{\text{PED}'}(0,0) = \beta\lambda \int_{-r_E}^0 \int_{\sqrt{r_E^2 - x^2}}^{Y_N - \frac{2\sqrt{3}}{2}r_E} \frac{dx dy}{x^2 + y^2}. \quad (11)$$

The numerical results of the total interference accumulated at $(0,0)$ by applying the above approximation are also illustrated in Fig. 8 with legend ‘‘Simplified’’. The difference between $P_{r,\text{HG}}^{\text{PED}}(0,0)$ and the simplified calculation is relatively small, therefore, we could have the following corollary to reduce the calculation complexity when possible.

Corollary 3. *When applying the PED-based method on a large network, the parameter S_E in (6) of Corollary 1, which represents the actual region occupied by an ER in the network,*

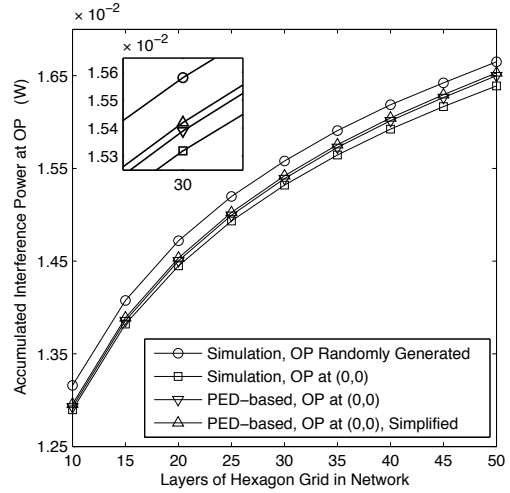


Fig. 8. Numerical and simulation results of rectangle network with hex-grid, (similarly, the randomly generated OP is on circle $x^2 + y^2 = \frac{1}{4}d_{t,r}^2$ in Fig. 7)

can be replaced by a disk with radius r_E .

Note that, in the two examples above, the network area was assumed to just fit the square/hexagon grid, which might not always happen in the real situation. For a more realistic modeling, we could slightly adjust the original network area to $(X_N + X_\Delta) \times (Y_N + Y_\Delta)$, where $X_\Delta < r_E$ and $Y_\Delta < \frac{\sqrt{3}}{3}r_E$ when the ERs are arranged in a hexagon grid, otherwise, more communication pairs could be arranged in. Intuitively, when the network area is relatively large, the additional X_Δ and Y_Δ will be ignorable for X_N and Y_N , respectively. Therefore, the accumulated interference at OP should still be calculated by adjusting the upper bounds in the integrals of (10). This observation is verified by the simulation results shown in Fig. 9, and summarized as Corollary 4.

Corollary 4. *For a large network with given a compact ER arrangement, the part of the network area near the network boundary, which cannot fit in half of a node pair’s ER, can be ignored for accumulated interference power calculation.*

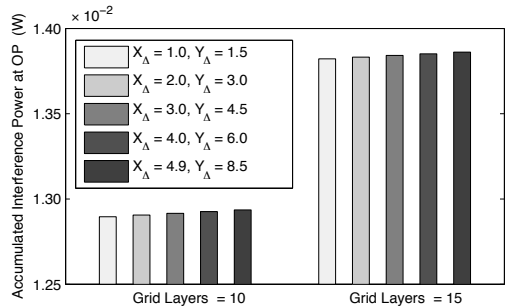


Fig. 9. Rectangle network with slightly increased X_Δ (m) and Y_Δ (m)

C. Disk Network Area with Hexagon Grid ERs

If we move one step forward by changing the network area from a rectangle to a disk, the accumulated interference power at an observed receiver, which is even more difficult to be

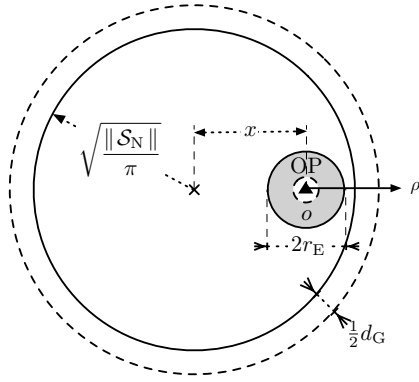


Fig. 10. Disk network with ERs arranged as a hexagon grid

solved by the discrete method, can also be obtained by the PED-based approach. Due to that the network nodes could be located on the boundary of the designated network area, the actual area to arrange the ERs is a disk with radius $R = \sqrt{\frac{\|S_N\|}{\pi}} + \frac{1}{2}d_G$ as shown in Fig. 10.

Suppose that the observed ER's center is located with distance x from the network area's center. According to Corollaries 2 to 4, the interference accumulated at the observed receiver can be approximated by the interference accumulated at the ER's center, the disk shaped ER could be used to simplify the calculation, and the area near the network boundary can be ignored. Therefore, by building up a polar coordinate system with its origin at the observed ER center, the accumulated interference power at the observed receiver, when all the ERs are arranged in the most compact way, could be easily calculated as

$$\begin{aligned}
 P_{r,C-HG}^{\text{PED}}(x) &= \beta \lambda \int_0^{2\pi} \int_{r_E}^{\sqrt{R^2 - x^2 \sin^2 \theta - x \cos \theta}} \frac{r \, dr \, d\theta}{r^2} \\
 &= \beta \lambda \int_0^{2\pi} \ln \frac{\sqrt{R^2 - x^2 \sin^2 \theta - x \cos \theta}}{r_E} \, d\theta \\
 &= \beta \lambda \pi \ln (R^2 - x^2) - 2\beta \lambda \pi \ln r_E \quad . \quad (12)
 \end{aligned}$$

Based on (12), the accumulated interference at the observed receiver reaches the maximum when $x = 0$ (the ER's center is coincident with the network area's center), and reduces to the minimum when $x = R - \frac{1}{2}d_G$ (the ER's center is on the boundary of the network area). Due to the space limit, the evaluation results are not shown here.

V. A BRIEF DISCUSSION

Once we verified the accuracy of the proposed PED-based method, a lot of interesting topics can be investigated in a quite direct and concise way. For example, by combining the required Signal to Interference Ratio (SIR) threshold at a receiver, the guard distance d_G for guaranteeing an expected maximum outage probability γ could be easily obtained. By setting the minimum communication distance of a node pair d_{\min} , which represents the minimum physical separation between two network terminals (e.g., 1 m), SIR at a receiver in both the worst and least interfered cases can be derived, and

then the upper and lower capacity bounds of a single node pair could also be directly obtained according to the Shannon's channel capacity theorem. Besides, the PED method itself could still be further evolved. For example, results for more general path loss exponent η should be obtained for convenient. Moreover, all the ERs in the network, which are assumed to be identical currently, could be described by a more realistic heterogeneous model; the medium access control model, which is ignored in the current results, can be added as a determining factor of ER's distribution for more specific research issues. All these interesting topics will be studied in our future work.

VI. CONCLUSIONS

In this paper, we have proposed a Power Emission Density-based interference calculation method for random wireless networks. By theoretical analysis and simulation validation, the accuracy of our method had been verified. Comparing with the traditional discrete-style method, the new method's calculation complexity is greatly reduced. Moreover, some insights are also provided for the possible applications and improvements of the PED-based method.

ACKNOWLEDGMENT

This work is partly supported by NSERC, CFI, BCKDF (with contributions from CRC and DRDC), China Postdoctoral Science Foundation (Grant No. 2013M540847), the Fundamental Research Funds for the Central Universities (Grant No. 2014JBM154), and the State Key Laboratory of Rail Traffic Control and Safety (Grant No. RCS2014ZQ003), and NSFC (Grant No. U1334202).

REFERENCES

- [1] M. Haenggi and R. K. Ganti, "Interference in large wireless networks," *Foundations and Trends in Networking*, vol. 3, no. 2, pp. 127–248, 2009.
- [2] P. Cardieri, "Modeling interference in wireless ad hoc networks," *IEEE Commun. Surveys Tuts.*, vol. 12, no. 4, pp. 551–572, Oct. 2010.
- [3] A. Baddeley, "Spatial point processes and their applications," Springer, Oct. 2006.
- [4] J. Andrews, S. Shakkottai, R. Heath, N. Jindal, M. Haenggi, R. Berry, D. Guo, M. Neely, S. Weber, S. Jafar, and A. Yener, "Rethinking information theory for mobile ad hoc networks," *IEEE Commun. Mag.*, vol. 46, no. 12, pp. 94–101, 2008.
- [5] J. Venkataraman, M. Haenggi, and O. Collins, "Shot noise models for the dual problems of cooperative coverage and outage in random networks," in *Proc. of 44th Annual Allerton Conf.*, 2006, pp. 709–718.
- [6] M. Haenggi, J. G. Andrews, F. Baccelli, O. Dousse, and M. Franceschetti, "Stochastic geometry and random graphs for the analysis and design of wireless networks," *IEEE J. Sel. Areas Commun.*, vol. 27, no. 7, pp. 1029–1046, 2009.
- [7] M. Haenggi, "Outage and throughput bounds for stochastic wireless networks," in *Proc. of IEEE ISIT*, 2005, pp. 2070–2074.
- [8] P. Gupta and P. R. Kumar, "The capacity of wireless networks," *IEEE Trans. Inf. Theory*, vol. 46, no. 2, pp. 388–404, 2000.
- [9] L. G. Roberts, "ALOHA packet system with and without slots and capture," *ACM Computer Commun. Rev.*, vol. 5, pp. 28–42, 1975.
- [10] Y. Yu, X. Cai, and G. B. Giannakis, "On the instability of slotted Aloha with capture," in *Proc. of IEEE WCNC*, 2004, pp. 728–732.
- [11] Wikipedia, "Shell Theorem," [Online]. http://en.wikipedia.org/wiki/Shell_theorem.
- [12] K. Stephenson, "Circle packing: a mathematical tale," *Notices Amer. Math. Soc.*, vol. 50, pp. 1376–1388, 2003.
- [13] A. Jeffrey and D. Zwillinger, *Table of integrals, series, and products*, 7th ed. Academic Press, Feb. 2007.